JOC The Journal of Organic Chemistry

Article

pubs.acs.org/joc

NMR Spectroscopic and Computational Study of Conformational Isomerism in Substituted 2-Aryl-3*H*-1-benzazepines: Toward Isolable Atropisomeric Benzazepine Enantiomers

Keith Ramig,*[,†] Edyta M. Greer,*[,†] David J. Szalda,[†] Sasan Karimi,[‡] Allen Ko,[†] Laura Boulos,[†] Jiansan Gu,[†] Nathan Dvorkin,[†] Hema Bhramdat,[§] and Gopal Subramaniam*[,§]

[†]Department of Natural Sciences, Baruch College of the City University of New York, 17 Lexington Avenue, New York, New York 10010, United States

[‡]Department of Chemistry, Queensborough Community College of the City University of New York, 222-05 56th Avenue, Bayside, New York 11364, United States

[§]Department of Chemistry and Biochemistry, Queens College of the City University of New York, 65-30 Kissena Boulevard, Flushing, New York 11367, United States

Supporting Information

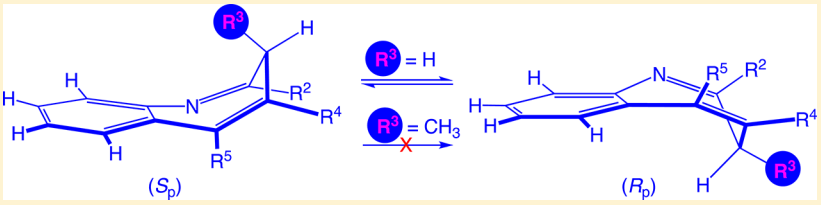

ABSTRACT: Certain 2-aryl-3*H*-1-benzazepines are conformationally mobile on the NMR time scale. Variable-temperature NMR experiments bolstered by calculations indicate that alkylation of the azepine ring will slow the interconversion of conformational enantiomers markedly. DFT studies show that, while the substitution patterns of the aryl groups at C2 and C4 do not exert large effects on the rate of enantiomerization, alkylation at C5 slows it appreciably. Alkylation at C3 slows enantiomerization even more, possibly to the extent that isolation of atropisomers might be attempted.

INTRODUCTION

The 3*H*-azepine molecule is nonplanar, by virtue of its lone sp^3-hybridized carbon atom. Since the nitrogen atom breaks symmetry, the molecule exhibits the planar form of chirality,[1] even though it lacks a chiral center. Enantiomerization by conformational exchange (a ring-flip) in this system is facile even at low temperature, so the two enantiomers are inseparable from each other. This has been determined from NMR studies of the ring-flip of various derivatives, where the energy barriers to enantiomerization range from 10 to 16 kcal/mol.[2−5] There have been two brief reports on the enantiomerization of their benzo-fused derivatives, 3*H*-1-benzazepines. Brooke and Matthews[6] have reported the synthesis and fluxional properties of the highly fluorinated 3*H*-1-benzazepines **1a** and **1b** (Scheme 1; stereochemical descriptors are assigned using the formalism of Eliel and Wilen[7]). They noted that the two protons at C3 in **1a** appear as a two-proton singlet in the NMR spectrum at room temperature. This is an indication that enantiomerization is rapid in this system. Upon lowering the temperature to −20 °C, the singlet became two very broad one-proton signals. For **1b**, however, the protons at C3 each show a broad doublet at room temperature, and the doublets persist up to 37 °C, the highest temperature used in that study. Although the energy barriers to enantiomerization were not calculated, it is obvious that **1b** has the higher of the two. The high energy barrier in **1b** may be attributed to steric interactions between the fluorine atom at C12 and the proton at C5 developing in the transition state of the ring-flip.

Scheme 1. Enantiomerization of Benzazepine 1 by Conformational Exchange

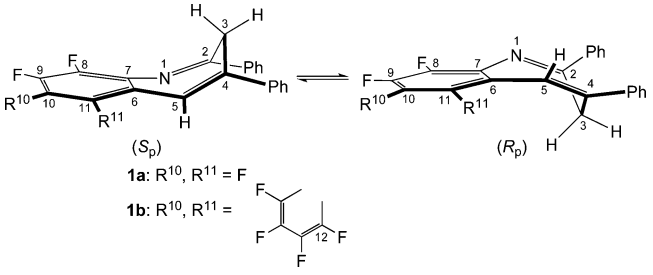

The other study[8] on the enantiomerization of 3*H*-1-benzazepines comes from our laboratories. That study dealt primarily with the synthesis and mechanism of formation of benzazepines **2a−2c** and other benzazepines. We found that the NMR signal-coalescence temperature of the C3 protons in

Received: June 17, 2013
Published: July 12, 2013

2,4-diphenyl-3*H*-1-benzazepine (**2a**) is much lower than that in its 5-alkyl derivatives **2b** and **2c** ((S_p) isomers are shown arbitrarily). We inferred that the activation-energy barrier to enantiomerization in the alkyl derivatives **2b** and **2c** must be higher than that in the parent **2a**. The explanation for this could be due to steric interactions involving groups near the ring juncture. In the derivatives alkylated at C5, the alkyl group and the hydrogen atom at C11 must pass closely by each other during enantiomerization, which would presumably raise the energy barrier.

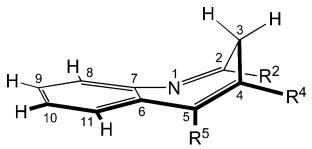

2a: R^2=Ph, R^4=Ph, R^5=H
2b: R^2=*p*-MePh, R^4=Ph, R^5=Me
2c: R^2=*p*-MePh, R^4,R^5=$(CH_2)_4$

Although 1-benzazepines have been little studied, the structurally related 1,4-benzodiazepines, which are important pharmaceutical compounds, have received much attention. A comparison of benzazepine **2a** and a typical benzodiazepine, desmethyldiazepam (**3a**), highlights their similarity. Both exhibit planar chirality by virtue of seven-membered rings that are puckered into boatlike conformations. This close similarity makes it not surprising that the protons on C3 in both molecules appear as two-proton singlets in their proton NMR spectra at room temperature.[9,10] If ring-flipping were slow or not occurring, then each proton would be a doublet, as they would experience geminal coupling; diazepam (**3b**) exhibits this feature in its NMR spectrum at room temperature.[10] These phenomena were first noted for benzodiazepines by Linscheid and Lehn, who used NMR signal-coalescence measurements to determine energy barriers to enantiomerization.[11] A series of NMR experiments and calculations studying this conformational isomerism then appeared.[12−17] In general, the conformational exchange of benzodiazepines is too fast for the individual enantiomers to be isolated, although, in some cases, with especially rigid structures, they can be separated by chiral HPLC.[18] Studies of conformational enantiomerism continue to be important, because it has been noted that enzymes in the body can distinguish between the conformational enantiomers of benzodiazepines.[10,19,20]

Bulky groups near the ring juncture of the benzodiazepine system raise the energy barrier to enantiomerization, sometimes imparting sufficient stability for the individual atropisomers to be isolated and studied. A comparison of benzodiazepines **3a**, **3b**, and **3c** shows that, as the steric bulk of the N1 substituent increases, so does the activation-energy barrier (Table 1). This is because the groups on opposite sides of the ring juncture become close to each other in the planar transition state of the interconversion, causing steric repulsion. In **3d**, where N1 bears a *t*-butyl group, the ring-flip is slow enough to allow resolution of the enantiomers.[21] The energy barrier in this case was estimated to be at least 24 kcal/mol, which appears to be the lower limit for handling the individual isomers at room temperature without appreciable racemization. When two methyl groups are at opposite sides of the ring juncture, as in **3f**, the steric repulsion is even greater.[17]

Below, we report the application of NMR signal-coalescence techniques and DFT calculations to the study of enantiomerization by conformational exchange in a series of 3*H*-1-benzazepines. The 1-benzazepine moiety with various substitution patterns and saturation levels is an important substructure found in many pharmacologically active molecules.[22−25] In some cases, these molecules and closely related ones that are also chiral exhibit atropisomerism.[26−29] Two stereoisomeric conformers are considered atropisomers if interconversion by rotation around single bonds is slow enough to allow their separation and characterization.[30] Determining the atropisomeric properties of a molecule is important, as it is becoming clear that enantiomerism based on changes in both planar and axial chirality has an important bearing on the biological activity of chiral molecules in general,[31] not just in the benzodiazepines mentioned above. Our studies are aimed at designing a benzazepine that is conformationally rigid enough to allow isolation of the stereoisomers. This would unveil previously inaccessible planar-chiral benzazepines, which may lead to new single-enantiomer benzazepine drug candidates.

RESULTS AND DISCUSSION

Seven benzazepines were chosen for the NMR study (Table 2). Benzazepines **2a**,[9] **2b**,[8] **2c**,[8] and **2d**[32] are known compounds, and were obtained by literature procedures. The (5-methyl-2-furyl)-substituted benzazepine **2e** was prepared by condensation of 2-fluoroaniline with 2-acetyl-5-methylfuran (Scheme 2).[32] The 4-(*o*-toluyl)-substituted benzazepine **2f** was synthe-

Table 1. Energy Barriers to Enantiomerization of Benzodiazepines from the Literature

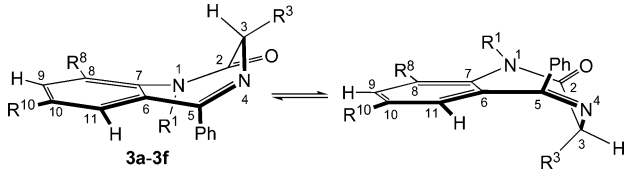

3a-3f

cpd	R^1	R^3	R^8	R^{10}	T_c[a] (°C)	$\Delta G^{\ddagger}_{exp}$[b] (kcal/mol)	$\Delta G^{\ddagger}_{calc}$[c] (kcal/mol)
3a	H	H	H	Cl	−20	12.3[d]	10.7−11.3[e]
3b	Me	H	H	Cl	118	18[f]	16.8−17.6[f]
3c	*i*-Pr	H	H	Cl	>185	>21.3[f]	20.2−21.6[f]
3d	*t*-Bu	H	H	Cl	>100	>24[g]	
3e	H	Me	H	Cl			12.5−12.8[e]
3f	Me	H	Me	Me	>180	25.1[h]	26.3[h]

[a]NMR signal-coalescence temperature of the protons of the C3 methylene group. [b]Experimental Gibbs free energy of activation. [c]Calculated Gibbs free energy of activation. [d]Reference 11. [e]Reference 13. [f]Reference 15. [g]Reference 21. [h]Reference 17.

dx.doi.org/10.1021/jo4013089 | J. Org. Chem. 2013, 78, 8028−8036

Table 2. NMR Signal-Coalescence Temperatures and Corresponding Enantiomerization Activation Parameters of 3*H*-1-Benzazepines 2a−2f

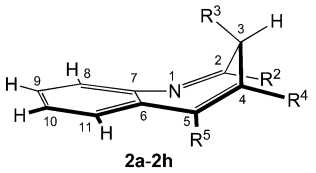

2a-2h

2a R^2 = Ph, R^3 = H, R^4 = Ph, R^5 = H
2b R^2 = *p*-MePh, R^3 = H, R^4 = Ph, R^5 = Me
2c R^2 = *p*-MePh, R^3 = H, R^4,R^5 = $(CH_2)_4$
2d R^2 = 2-naphthyl, R^3 = H, R^4 = 2-naphthyl, R^5 = H
2e R^2 = 5-Me-2-furyl, R^3 = H, R^4 = 5-Me-2-furyl, R^5 = H
2f R^2 = *p*-MePh, R^3 = H, R^4 = *o*-MePh, R^5 = H
2g R^2 = Ph, R^3 = Me, R^4 = Ph, R^5 = H
2h R^2 = Ph, R^3 = H, R^4 = Ph, R^5 = *t*-Bu

cpd	T_c[a] (K)	solvent	$\Delta G^{\ddagger}$[b] (kcal/mol)	$\Delta H^{\ddagger}$[c] (kcal/mol)	$\Delta S^{\ddagger}$[d] (cal/K·mol)	E_a[e] (kcal/mol)
2a	233	acetone-d_6	9.9 ± 0.2	9.6 ± 0.2	−1.8 ± 0.7	9.9 ± 0.2
2b	323	benzene-d_6	14.2 ± 0.2	12.7 ± 0.2	−4.8 ± 0.6	13.3 ± 0.2
2c	323	benzene-d_6	14.3 ± 0.2	12.8 ± 0.3	−5.0 ± 0.7	12.8 ± 0.3
2d	248	acetone-d_6	10.6 ± 0.2	9.5 ± 0.4	−4.0 ± 1.5	9.9 ± 0.4
2e	223	acetone-d_6	9.6 ± 0.2	8.3 ± 0.2	−4.9 ± 0.7	8.8 ± 0.2
2f	228	acetone-d_6	9.8 ± 0.2	8.7 ± 0.2	−4.3 ± 1.4	8.9 ± 0.3
2g	[f]	DMSO-d_6	[f]	[f]	[f]	[f]

[a]NMR signal-coalescence temperature of the protons of the C3 methylene group. In all compounds, the location of the signal due to the methylene protons at C3 was confirmed by NOE to the adjacent substituents at the 2- and 4-positions. [b]Gibbs free energy of activation. Values calculated from the rate constants obtained from T_c measurements, and those obtained from Eyring plots, are identical within the error limits. [c]Activation enthalpy. [d]Activation entropy. [e]Arrhenius activation energy. [f]There was no change in the NMR spectrum up to 373 K, the temperature limit of the probe used.

Scheme 2. Synthesis of (5-Methyl-2-furyl)-Substituted Benzazepine 2e

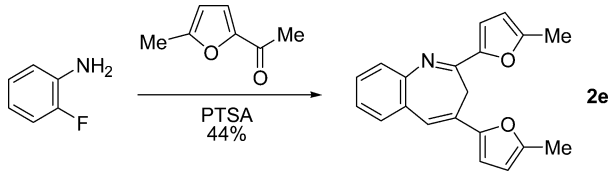

sized in three steps from the trimethylsilyl enol ether of 4′-methylacetophenone (**4**), 2′-methylacetophenone, and 2-fluoroaniline (Scheme 3).[8,33,34] The 3-methyl-substituted

Scheme 3. Synthesis of 4-(*o*-Toluyl)-Substituted Benzazepine 2f

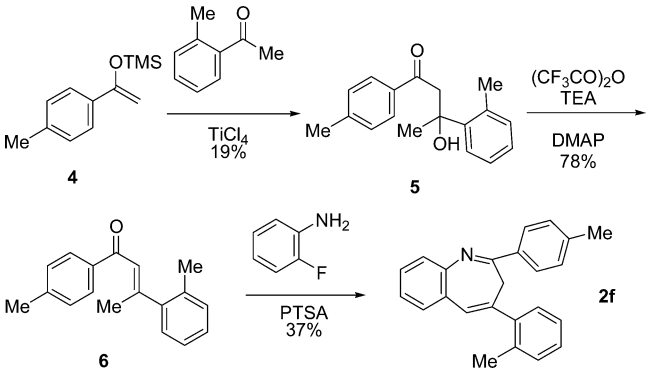

benzazepine **2g** was prepared by deprotonation of benzazepine **2a** with LDA, followed by alkylation of the presumed anion with methyl iodide (Scheme 4). This procedure was suggested

Scheme 4. Synthesis of 3-Methyl-Substituted Benzazepine 2g

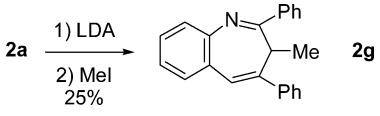

by the work of Streef and van der Plas, who alkylated 3*H*-azepines at C3 in a similar fashion.[35] NMR analysis of the crude reaction mixture containing benzazepine **2g** showed only one of the two possible diastereomers. The pseudoaxial disposition of the methyl group is indicated by the X-ray crystal structure (Figure 1).

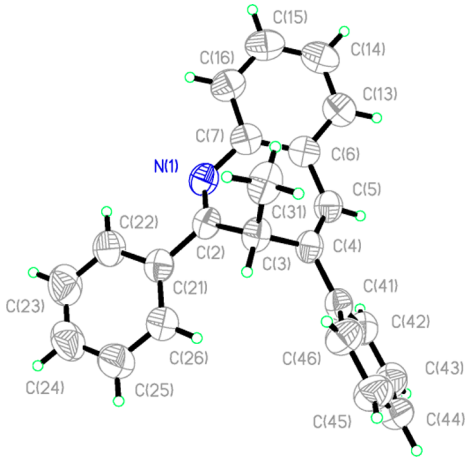

Figure 1. ORTEP diagram of benzazepine **2g** ((R_p) (3*R*) enantiomer shown).

NMR Spectroscopic Study of the Enantiomerization Process. Table 2 shows the energy barriers to enantiomerization along with error estimates, from experimental NMR measurements of the protons at C3 as a function of temperature. For example, at room temperature, the broadened singlet due to the protons at C3 in phenyl-substituted **2a** appears at 3.38 ppm.[9] At lower temperatures, these protons appear as two doublets. Coalescence occurs at −40 °C. The Gibbs free energy of activation ($\Delta G^{\ddagger}$) at the coalescence temperature was calculated from the coalescence temperature (T_c),[36] and the error limits were estimated using an uncertainty of ±3 K in the measurement of coalescence temperatures. The Arrhenius activation energy (E_a) was calculated in a similar fashion (details are in the Experimental Section and the

dx.doi.org/10.1021/jo4013089 | J. Org. Chem. 2013, 78, 8028−8036

Table 3. Computed Dihedral Angles and Enantiomerization Activation Parameters of 3*H*-1-Benzazepines 2a−2h

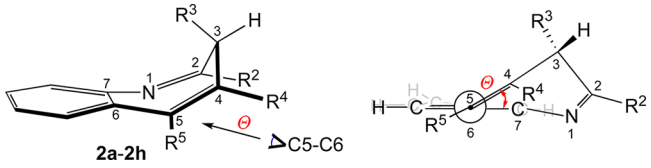

cpd	Θ[a] (deg)	$\Delta G^{\ddagger}$[b] (kcal/mol)	$\Delta H^{\ddagger}$[c] (kcal/mol)	$\Delta S^{\ddagger}$[d] (cal/K·mol)	E_a[e] (kcal/mol)
2a	31.5	9.8	8.8	−3.1	9.2
2b	37.1 (40.7)[f]	14.0	12.5	−5.0	13.0
2c	38.1	13.5	12.8	−2.5	13.1
2d	31.6	10.0	9.0	−3.4	9.3
2e	31.1	7.5	6.3	−3.9	6.7
2f	32.6	9.1	8.2	−3.0	8.5
2g	26.9 (28.8)[f]	16.4	15.2	−4.1	15.6
2h	49.3	26.0	24.6	−4.7	25.0

[a]C7−C6−C5−C4 dihedral angle. [b]Gibbs free energy of activation. [c]Activation enthalpy. [d]Activation entropy. [e]Arrhenius activation energy. [f]Value in parentheses was obtained from X-ray crystal data; for **2b**, see ref 8.

Supporting Information). As the coalescence temperatures for benzazepines **2a−2f** vary significantly, it was necessary to employ different deuterated solvents to access these temperatures in solution. The compounds with low T_c were studied in acetone-d_6, whereas those that exhibited higher coalescence temperatures were studied in benzene-d_6. Solvent viscosity can affect the experimental activation-energy values.[37] Though benzene is more viscous than acetone at room temperature, at the coalescence temperature of 50 °C, the viscosity of benzene is 0.442 cP, whereas that of acetone at −42.5 °C is 0.695 cP.[38] Because these values are similar to each other, the deviations in E_a coming from viscosity changes due to temperature are expected to be small.

The $\Delta G^{\ddagger}$ values were also determined from the Eyring plots,[39] which gave the activation enthalpies ($\Delta H^{\ddagger}$) and activation entropies ($\Delta S^{\ddagger}$). We found that this method gave $\Delta G^{\ddagger}$ values that matched those from the coalescence temperature measurements described above. Table 2 shows that $\Delta S^{\ddagger}$ values are very small, in the range of −1.8 to −5.0 cal/K·mol. The dominating activation-enthalpy terms clearly point to a free-energy barrier arising primarily from potential energy constraints for achieving the transition state.

Comparison of phenyl-substituted **2a**, (2-naphthyl)-substituted **2d**, (5-methyl-2-furyl)-substituted **2e**, and 4-(*o*-toluyl)-substituted **2f** shows that the nature of the aryl groups at C2 and C4 has only a small effect on the energy barrier to ring-flip. Benzazepine **2f** contains an axis of chirality (the C4-phenyl-C bond), which is a consequence of the presence of the *ortho* methyl group on the phenyl group at C4. (Also, two axes of chirality exist in both (2-naphthyl)-substituted **2d** and (5-methyl-2-furyl)-substituted **2e**; the consequences of this will be discussed later.) This *ortho* methyl group might be expected to hinder rotation of the phenyl group during the ring-flip, or even cause the molecule to exist as a mixture of diastereomers if the rotation around the axis of chirality is slow enough. An effect of this sort has been noted in benzodiazepines substituted with the 2-fluorophenyl group.[40,41] The full enantiomerization process for 4-(*o*-toluyl)-substituted **2f** consists of changes in both types of chirality, planar and axial. However, the experimental energy barrier in this case is lower than that of phenyl-substituted **2a**, so the barrier to rotation around the C4-phenyl-C bond must be lower than the barrier to the ring-flip. The NMR spectra of **2f** at all the temperatures studied shows only changes associated with the ring-flip; no evidence for the presence of diastereomers, or any other change in the signals for the other protons, was seen.

The relatively high energy barriers in 5-methyl-substituted **2b** and butylene-substituted **2c** are most likely due to the steric repulsion engendered by passage of the C5 alkyl group and the C11 hydrogen atom by each other during the ring-flip. A direct analogy can be drawn between these cases and the benzodiazepines **3a−3d** (see Table 1). This situation is also similar to the case of fluorinated benzazepine **1b** mentioned earlier, where increased steric bulk at C11 results in a much higher barrier to ring-flip.

The behaviors of 3-methyl-substituted benzazepine **2g** and 3-methyl-substituted benzodiazepine **3e** make an interesting comparison. The presence of the methyl group at C3 in benzodiazepine **3e** is calculated to add less than 2 kcal/mol to the ring-flip energy barrier (vs its 3-desmethyl derivative **3a**), while the preferred orientation of the methyl group is equatorial.[13,42,43] On the other hand, we believe that the flanking phenyl groups of 3-methyl-substituted **2g** cause its C3 methyl group to be axial, and inhibit the ring-flip greatly. The methyl group may suffer massive steric repulsions in the transition state of the ring-flip, and in the unobserved pseudoequatorial-methyl isomer.

Computational Study of the Enantiomerization Process. Gas-phase B3LYP/6-31G(d) calculations of activation parameters have been conducted for comparison to experimental values, and for unraveling the intricacies in the ring-flip processes, especially of 3-methyl-substituted benzazepine **2g**, (5-methyl-2-furyl)-substituted **2e**, and 4-(*o*-toluyl)-substituted **2f**. These three compounds contain complicating structural features that make explanation of trends in their ring-flip activation energies a challenge. Also, a 5-*t*-butyl-substituted benzazepine (**2h**) is proposed, with a barrier to inversion that may be high enough to allow separation and study of individual enantiomers. The data will show that increased boat character (puckering of the ring) in the azepine moiety corresponds to an increase in the inversion barrier in some cases. If this correspondence is a general phenomenon, then benzazepine enantiomers would be obtainable based on a sufficiently high degree of ring-puckering. This work relies heavily on the thorough studies of Carlier et al.,[14−17] who characterized the ring-flip of benzodiazepines both experimentally and computa-

dx.doi.org/10.1021/jo4013089 | J. Org. Chem. 2013, 78, 8028−8036

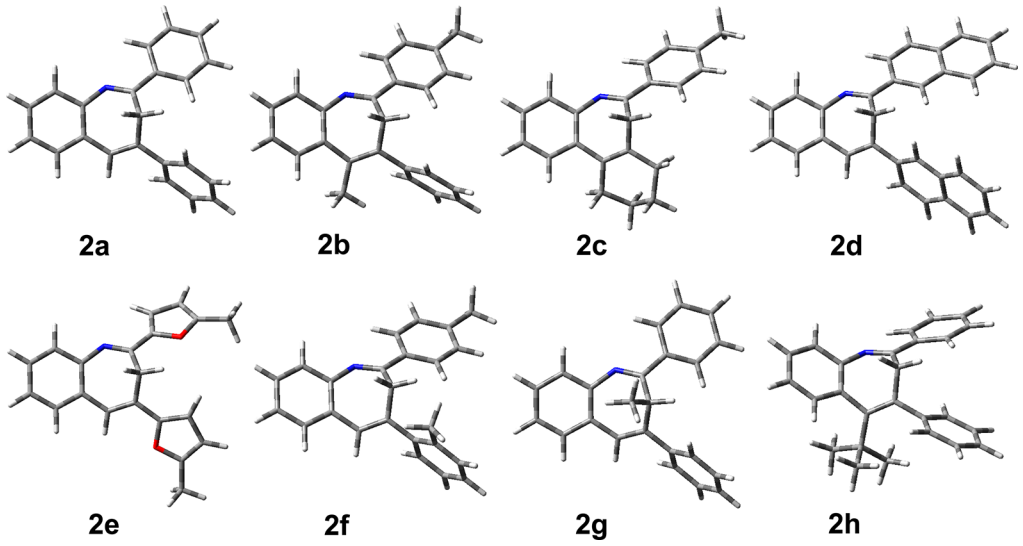

Figure 2. B3LYP/6-31G(d) optimized minima for benzazepines **2a**–**2h**.

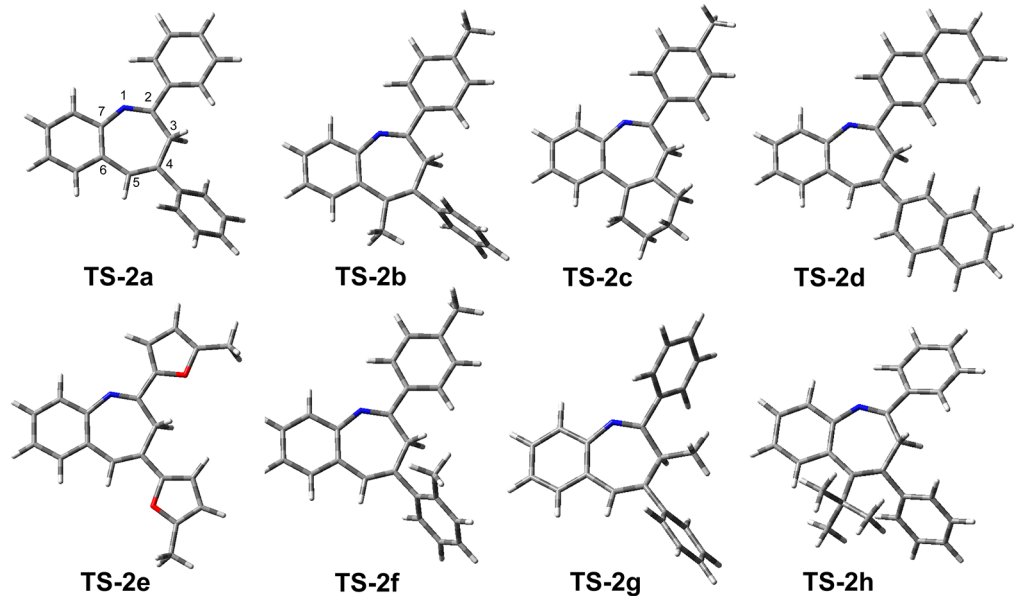

Figure 3. B3LYP/6-31G(d) calculated transition structures of **TS-2a** to **TS-2h**.

tionally, using the same basis set used here. Paizs and Simonyi[13] have also shown that this basis set reproduces experimental values best in these types of systems. Both of these research groups noted that solvent effects are negligible, so we believe our use of gas-phase calculations is justified.

Table 3 shows the computational activation data for all the benzazepines from Table 2 (plus *t*-butyl-substituted benzazepine **2h**, which was not synthesized) based on their global minimum-energy conformers. The structures of the lowest-energy conformers of benzazepines **2a**–**2h** are displayed in Figure 2. (See the Supporting Information for full structural parameters.) The transition structures were determined by gradually constraining dihedral angles in the azepine rings of benzazepines **2a**–**2h**, followed by unconstrained optimization. The transition-state geometries were verified by one imaginary frequency corresponding to the displacement vectors distorting the planar or nearly planar geometry of the transition states. Wherever possible, intrinsic reaction coordinate (IRC) calculations were also used to verify the transition-state structures.

Transition-state structures are shown in Figure 3. Interestingly, not all of these are planar. Transition-state structures **TS-2a**, **TS-2c**, **TS-2d**, **TS-2f**, **TS-2g**, and **TS-2h** deviate in differing degrees from planarity. Whereas structures **TS-2a**, **TS-2c**, **TS-2d**, **TS-2f**, and **TS-2h** are situated closer to the (S_p) reactants, structure **TS-2g** is closer to the (R_p) product. (See the Supporting Information for full structural parameters.) Similarly, Lam and Carlier[15] and Paizs and Simonyi[13] have found nonplanar transition-state structures in the enantiomerization process of benzodiazepines. This deviation from planarity indicates that the interconversion of (R_p) and (S_p) enantiomers occurs via two equienergetic pathways, which pass through one of two enantiomeric transition states.

The computed values of Table 3 compare well with the experimental values of Table 2, except in the case of (5-methyl-2-furyl)-substituted **2e**, which has a 24% difference between the experimental and theoretical values of E_a. The theoretical

dx.doi.org/10.1021/jo4013089 | *J. Org. Chem.* 2013, 78, 8028–8036

treatment of this benzazepine is complicated by the presence of multiple similar ground-state conformers, engendered by the two axes of chirality introduced by the 5-methyl-2-furyl groups. The conformer of lowest energy was chosen as the basis for the calculation. The same is true for (2-naphthyl)-substituted **2d** and *o*-toluyl-substituted **2f**. (Details are available in the Supporting Information.)

Also included in Table 3 is the dihedral angle of C7−C6−C5−C4, designated as Θ. A large Θ value indicates a highly puckered azepine ring. The data indicate that, in certain cases, there is a strong dependence of E_a on changes in Θ. Thus, it appears that a highly puckered azepine ring results in a large E_a. The Θ values for phenyl-substituted **2a**, (2-naphthyl)-substituted **2d**, and (5-methyl-2-furyl)-substituted **2e**, however, are identical within the error limits of the computational method, and Θ for *o*-toluyl-substituted **2f** differs by about a degree. Although the degrees of puckering for these four are identical or nearly so, the E_a values vary markedly, in a way that is difficult to rationalize. The molecules differ from each other only in the steric bulk of the aryl groups at C2 and C4. The (5-methyl-2-furyl)-substituted **2e** has the smallest aryl groups; thus, if steric interactions with the azepine ring are important, it may be expected to have the lowest E_a. Next is phenyl-substituted **2a**; the larger phenyl groups may cause a higher E_a. The (2-naphthyl)-substituted **2d** has the largest aryl groups, but much of the steric bulk is situated far away from the azepine ring. Thus, it behaves like phenyl-substituted **2a**. The *o*-toluyl-substituted **2f** bucks this trend entirely. The methyl group of the *o*-toluyl group might be expected to interact strongly with the azepine ring during the ring-flip, yet its E_a is the second lowest.

o-Toluyl-substituted **2f**, as mentioned earlier, has an axis of chirality. Thus, the full enantiomerization process includes a ring-flip and a rotation about the axis of chirality. The rotation can occur in two ways, with the methyl group passing by either the C5 hydrogen atom or the C3 hydrogen atoms. We have modeled this process both for the ground-state geometry (Figure 2) and for the transition state **TS-2f** (Figure 3). We found that rotation past the C5 hydrogen atom is more energetically favorable than the alternative rotation, by 4 kcal/mol (see the Supporting Information for details). Since the methyl group passes by the C5 hydrogen atom with a barrier of 6 kcal/mol, and this barrier is smaller than that of the ring-flip (8.5 kcal/mol), no evidence of the rotation is seen in the variable-temperature NMR spectrum.

The benzazepines with alkyl groups at C5, 5-methyl-substituted **2b**, butylene-substituted **2c**, and 5-*t*-butyl-substituted **2h**, present a clearer relationship between steric bulk and E_a. Here, due to steric interactions of the C5 alkyl group with the C11 hydrogen atom, the azepine rings are highly puckered, and the puckering varies regularly with the size of the alkyl groups. The dihedral angles in the global-minimum geometries of 5-methyl-substituted **2b** and butylene-substituted **2c** are 37.1° and 38.1°, respectively; the predicted E_a values for them are 13.0 and 13.1 kcal/mol, respectively. The 5-*t*-butyl derivative **2h** is highly puckered, with a dihedral angle of 49.3°. The ring-flip is predicted to proceed via **TS-2h**, where the azepine ring is significantly distorted from planarity, making its geometry closer to the (S_p) reactant. The barrier for racemization of 5-*t*-butyl derivative **2h** observed computationally is 25.0 kcal/mol, which is the highest barrier of the series of benzazepines **2a**−**2h**. This value is in line with that for the *t*-butyl-substituted benzodiazepine **3d** from Table 1, which appears to have a free-energy barrier to ring-flip greater than 24 kcal/mol.[21] The high barrier of **3d** has allowed its individual enantiomers to be synthesized and studied without interconversion.[21] We expect that this property observed in the benzodiazepine series will hold for the benzazepines as well; that is, the installation of a bulky substituent near the ring juncture (C5) should be a generally effective way to enhance the racemization barrier. The synthesis of 5-*t*-butyl-substituted benzazepine **2h**, and other C5-substituted benzazepines, in their enantiomerically pure forms will be the subject of future work.

The 3-methyl derivative **2g** is the most vexing computationally and the most interesting experimentally. It is the benzazepine whose (R_p) and (S_p) isomers are most likely to be separable without isomerization. Those isomers are separated by **TS-2g**, the transition structure for the ring-flip, shown in Figure 3. Saddle point **TS-2g** is a transition structure as it bears one imaginary frequency. The visualization of this frequency shows the displacement vectors in **TS-2g** engaged in *out*-of-plane motion of the methyl group at C3, to achieve the minimum geometry of benzazepine **2g** shown in Figure 2. These motions are accompanied by rotation of the phenyl groups at C2 and C4 away from the emerging methyl group. On the basis of this data, benzazepine **2g** is too sterically congested for easy passage of the methyl group past the phenyl groups. The seven-membered ring in **TS-2g** is significantly distorted from planarity, and its geometry is reminiscent of the ring-flip product.

Calculations were performed to judge the relative stabilities of (S_p)-(3*S*)-**2g** and its ring-flipped diastereomer (R_p)-(3*S*)-**2g**. A ΔG° of 4.2 kcal/mol was found, in favor of (S_p)-(3*S*)-**2g**. Since its ring-flipped diastereomer is of much higher energy, one would expect an equilibrium ratio of 1400:1 at 20 °C favoring (S_p)-(3*S*)-**2g**; thus, it should be of high diastereomeric purity, existing almost exclusively as a pair of noninterconvertible enantiomers.

■ CONCLUSION

In our efforts to make conformationally stable stereoisomers of 3*H*-1-benzazepine derivatives for pharmacological applications, we investigated their fluxional behavior by varying substituents at C2, C3, C4, and C5, and analyzing the temperature dependences of their ^{1}H NMR spectra. The rate of exchange between the conformational enantiomers did not depend strongly on the size of the substituents at C2 and C4, and was rapid at room temperature. Activation energies obtained from variable-temperature NMR data varied from 8.8 to 9.9 kcal/mol. A simple methyl substitution at C5 slowed the exchange and increased the coalescence temperature by about 100 °C, giving an activation energy of 13.3 kcal/mol. Theoretical calculations of activation energy agreed with these experimental values. It is suggested that two forms of substitution can slow ring-flipping appreciably, thus opening the possibility of isolating pure stereoisomers: placing either a *t*-butyl group at C5 or a methyl group at C3 in the pseudoaxial orientation. In the former case, the calculated energy barrier to the ring-flip is 25 kcal/mol, high enough for possibly separating and studying the two enantiomers. In the latter case, namely, a pseudoaxial methyl group at C3, the ^{1}H NMR spectrum did not show the presence of the conformational diastereomer. Calculations revealed that the free-energy difference between the two diastereomers is 4.2 kcal/mol, in favor of the isomer with the

dx.doi.org/10.1021/jo4013089 | J. Org. Chem. 2013, 78, 8028−8036

pseudoaxial methyl group. This high value results in the presence of a negligible amount of the other isomer.

EXPERIMENTAL SECTION

Calculation of Activation Parameters. The rate of exchange, k, between the pseudoaxial and pseudoequatorial protons was measured as a function of absolute temperature, T, and ln k was plotted against $1/T$ and fitted to a straight line (see the Supporting Information for plots). The Arrhenius activation energy, E_a, was calculated from the slope of the fitted straight line. Similarly, ln k/T was plotted against $1/T$ and fitted to a straight line to obtain the value of $\Delta H^{\ddagger}$ from the slope and $\Delta S^{\ddagger}$ from the y intercept using the Eyring equation.[39] To estimate the error range in the experimental values for E_a, $\Delta H^{\ddagger}$, and $\Delta S^{\ddagger}$, these values were calculated using the fitted equation for all temperatures to calculate the lower and upper bounds. The $\Delta G^{\ddagger}$ values obtained from the Eyring plots and those obtained from coalescence temperature measurements[36] agreed with each other, within the error limits.

Computational Methodology. Calculations were performed with Gaussian 09.[44] Calculations were conducted using DFT with the exchange-correlation of B3LYP along with the 6-31G(d) basis set. B3LYP/6-31G(d) performed well based on the structural features reproduced for **2g** obtained via X-ray crystallography as well as X-ray data of other benzazepines. The optimizations were carried out in the gas phase, because previous calculations by Lam and Carlier[15] showed that the gas-phase barriers are well-reproduced in DMSO.

Collection, Reduction, and Refinement of X-ray Data. A crystal (0.50 × 0.50 × 0.40 mm) of $C_{23}H_{19}N$ (**2g**) was cut from a large cluster of crystals and mounted on a glass fiber. Diffraction data for **2g** indicated an orthorhombic symmetry and systematic absences consistent with space groups *Aba2* and *Cmna*. Space group *Aba2* was used for the solution and refinement of the structure based on *E* statistics. Crystal data and information about the data collection are provided in the Supporting Information. The structure of **2g** was solved[45] by direct methods. Each crystal contains both optical isomers. Since Mo radiation was used for the collection of intensity data, the absolute structure could not be reliably determined, so Friedel pairs were averaged for the refinement of the structure. There is one molecule of **2g** in the asymmetric unit. In the least-squares refinement,[45] anisotropic temperature parameters were used for all the non-hydrogen atoms. Hydrogen atoms were placed at calculated positions and allowed to "ride" on the atom to which they were attached. The isotropic thermal parameter for the hydrogen atoms in the structure were determined from the atom to which they were attached.

2,4-Di(5-methyl-2-furyl)-3*H*-1-benzazepine (2e). A solution of 2-fluoroaniline (0.65 mL, 6.7 mmol), 2-acetyl-5-methylfuran (0.83 g, 6.7 mmol), and *p*-toluenesulfonic acid monohydrate (40 mg) in 30 mL of *o*-xylene was heated at reflux under N_2 for 16 h in a Dean−Stark apparatus. After cooling to r.t., the solution was washed with 5% $NaHCO_3$ solution and dried over $MgSO_4$. Removal of the solvent under vacuum gave 1.03 g of crude product, which was purified by radial chromatography (silica gel, 20% EtOAc/hexane). Isolated was 0.45 g (44% yield) of **2e** as a yellow crystalline solid, mp 157−158 °C. ^{1}H NMR ($CDCl_3$, 400 MHz) δ 7.58 (dd, J = 8.1, 0.8 Hz, 1H) 7.46 (dd, J = 7.9, 1.2 Hz, 1H), 7.34 (dt, J = 1.6, 7.4 Hz, 1H), 7.21 (s,1H), 7.18 (dt, J = 1.2, 8.2 Hz, 1H), 7.01 (d, J = 3.3 Hz, 1H), 6.53 (d, J = 3.3 Hz, 1H), 6.12 (dd, J = 3.3, 0.9 Hz, 1H), 6.05 (dd, J = 3.0, 1.0 Hz, 1H), 3.09 (s, 2H), 2.39 (s, 3H), 2.34 (s, 3H); ^{13}C NMR ($CDCl_3$, 100 MHz) δ 156.5 (q), 153.0 (q), 151.9 (q), 151.0 (q), 147.2 (q), 146.6 (q), 130.5, 129.5 (q), 128.5, 126.7, 124.0 (q), 123.9, 121.8, 115.7, 108.7, 108.6, 107.9, 31.0 (CH_2), 14.2 (CH_3), 13.9 (CH_3); HRMS (CI-TOF) calcd. for $C_{20}H_{17}NO_2$ m/z 303.1254, found 303.1266.

2-(4-Methylphenyl)-4-(2-methylphenyl)-3*H*-1-benzazepine (2f). A solution of enone **6** (491 mg, 1.96 mmol), 2-fluoroaniline (0.380 mL, 3.92 mmol), and *p*-toluenesulfonic acid monohydrate (20 mg) in 25 mL *o*-xylene was heated at reflux under N_2 for 23 h using a Dean−Stark apparatus. The solution was cooled to r.t., and washed with 10 mL of 5% $NaHCO_3$. Drying over $MgSO_4$ and rotary evaporation gave 712 mg of an orange viscous oil. Purification by radial chromatography (silica gel, 2% EtOAc/hexane) gave 236 mg (37% yield) of benzazepine **2f** as a viscous yellow oil. ^{1}H NMR ($CDCl_3$, 400 MHz) δ 7.74 (d, J = 8.2 Hz, 2H), 7.66 (dd, J = 8.1, 1.2 Hz, 1H), 7.48 (dd, J = 8.1, 1.2 Hz, 1H), 7.45 (td, J = 8.1, 1.4 Hz, 1H), 7.30 (m, 2H), 7.26 (td, J = 7.9 and 1.4 Hz, 1H), 7.15−7.23 (m, 4H), 6.79 (s, 1H), 3.31 (s, 2H), 2.39 (s, 3H), 2.32 (s, 3H); ^{13}C NMR ($CDCl_3$, 100 MHz) δ 157.2 (q), 146.8 (q), 141.5 (q), 140.4 (q), 136.4 (q), 135.8 (q), 135.6 (q), 130.5, 130.2, 129.4 (q), 129.3, 129.2, 128.6, 128.2, 127.9, 127.8, 126.9, 125.9, 123.7, 36.8 (CH_2), 21.4 (CH_3), 20.5 (CH_3); HRMS (CI-TOF) calcd. for $C_{24}H_{21}N$ m/z 323.1669, found 323.1669.

2,4-Diphenyl-3-methyl-3*H*-1-benzazepine (2g). A solution of benzazepine **2a** (1.18 g, 3.99 mmol) and 40 mL of anhydrous THF was cooled to −68 °C, and LDA (4.0 mL, 2.0 M in THF/heptane/ethylbenzene, 8.0 mmol) was added dropwise, giving a dark-green solution. After 1 h, CH_3I (0.249 mL, 4.00 mmol) was added and the cold bath was removed. After 1.25 h at r.t., the yellow solution was partitioned between 30 mL of H_2O and 30 mL of Et_2O. Drying of the organic layer over $CaCl_2$ and rotary evaporation gave 1.31 g of crude product. Purification by radial chromatography (silica gel, 1% EtOAc/hexane) gave 309 mg (25% yield) of benzazepine **2g** as a yellow crystalline solid, mp 109−111 °C. Slow recrystallization from 20% EtOAc/hexane gave large hexagonal prisms suitable for X-ray crystallographic analysis. ^{1}H NMR ($CDCl_3$, 400 MHz) δ 7.86 (dd, J = 7.7, 1.8 Hz, 2H), 7.63 (d, J = 8.1 Hz, 1H), 7.55 (d, J = 8.1 Hz, 2H), 7.47 (dd, J = 8.0, 1.1 Hz, 1H), 7.34−7.44 (m, 7H), 7.23 (td, J = 7.6, 1.3 Hz, 1H), 7.09 (s, 1H), 5.00 (q, J = 7.2, 1H), 0.96 (d, J = 7.2 Hz, 3H); ^{13}C NMR ($CDCl_3$, 100 MHz) 160.6 (q), 146.0 (q), 142.0 (q), 140.3 (q), 139.7 (q), 130.4, 129.9, 128.7, 128.5, 128.1 (q), 128.0, 127.9, 127.8, 127.3, 127.1, 126.7, 124.0, 41.0 (CH), 12.3 (CH_3); HRMS (CI-TOF) calcd. for $C_{23}H_{19}N$ m/z 309.1512, found 309.1508.

3-Hydroxy-1-(4-methylphenyl)-3-(2-methylphenyl)butan-1-one (5). To a solution of $TiCl_4$ (13.2 mL, 1.0 M in CH_2Cl_2, 13.2 mmol) under N_2 was added an additional 5 mL of anhydrous CH_2Cl_2. The resulting solution was cooled to 2 °C, and a solution of 2′-methylacetophenone (1.75 mL, 13.2 mmol) in 4 mL of anhydrous CH_2Cl_2 was added dropwise, giving a yellow suspension. A solution of the trimethylsilyl enol ether of 4′-methylacetophenone[8] (2.72 g, 13.2 mmol) in 3 mL of anhydrous CH_2Cl_2 was added dropwise, giving a dark red cloudy mixture. This was warmed to r.t. and stirred for 1 h. The mixture was poured into 35 mL of rapidly stirred ice water. The organic layer was removed, and the aqueous layer was extracted with CH_2Cl_2 (2 × 10 mL). The three organic layers were combined and washed with 2 × 10 mL of 5% $NaHCO_3$ and once with 20 mL of brine. The organic layer was dried over $MgSO_4$ and suction-filtered through a short pad of silica gel. Rotary evaporation gave 1.86 g of a viscous yellow liquid. Purification by radial chromatography (silica gel, 5% EtOAc/hexane) gave 670 mg (19% yield) of aldol **5** as a viscous yellow liquid, R_f in 10% EtOAc/hexane = 0.27. ^{1}H NMR ($CDCl_3$, 400 MHz) δ 7.83 (d, J = 8.2 Hz, 2H), 7.34 (dd, J = 6.4, 2.0 Hz, 1H), 7.25 (d, J = 8.2 Hz, 2H,), 7.09 (m, 3H), 4.91 (s, 1H), 3.98 (d, J = 17.8 Hz, 1H), 3.28 (d, J = 17.8 Hz, 1H), 2.60 (s, 3H), 2.40 (s, 3H), 1.67 (s, 3H); ^{13}C NMR ($CDCl_3$, 100 MHz) δ 201.1, 144.7 (q), 144.3 (q), 135.3 (q), 134.5 (q), 132.9, 129.4, 128.2, 127.0, 125.7, 125.4, 75.0 (q), 47.9 (CH_2), 29.3 (CH_3), 22.5 (CH_3), 21.7 (CH_3); HRMS (CI-TOF) calcd. for $C_{18}H_{20}O_2$+H m/z 269.1536, found 269.1526.

(2*E*)-1-(4-Methylphenyl)-3-(2-methylphenyl)but-2-en-1-one (6). A solution of aldol **5** (193 mg, 0.719 mmol), triethylamine (0.430 mL, 3.09 mmol), and 4-(dimethylamino)pyridine (9 mg, 0.07 mmol) in 2 mL of anhydrous CH_2Cl_2 under N_2 was cooled to 0−5 °C. A solution of trifluoroacetic anhydride (0.200 mL, 1.44 mmol) in 2 mL of anhydrous CH_2Cl_2 was added dropwise. The resulting solution was warmed to r.t. and stirred for 20 h. The reaction solution was poured into 10 mL of rapidly stirred saturated Na_2CO_3 solution, and the resulting mixture was partitioned between 10 mL of H_2O and 10 mL of Et_2O. The organic layer was separated, and the aqueous layer was extracted with 10 mL of Et_2O. The two organic layers were combined and dried over $MgSO_4$. Rotary evaporation gave 200 mg of a viscous yellow oil. Purification by radial chromatography (silica gel, 5% EtOAc/hexane) gave 141 mg (78% yield) of enone **6** as a viscous

dx.doi.org/10.1021/jo4013089 | J. Org. Chem. 2013, 78, 8028−8036

yellow oil, R_f in 10% EtOAc/hexane = 0.50. ^{1}H NMR ($CDCl_3$, 400 MHz) δ 7.87 (d, J = 8.1 Hz, 2H), 7.25 (d, J = 8.1 Hz, 2H), 7.23−7.15 (m, 4H), 6.82 (q, J = 1.4 Hz, 1H), 2.48 (d, J = 1.4 Hz, 3H), 2.40 (s, 3H), 2.35 (s, 3H);^{13}C NMR ($CDCl_3$, 100 MHz) δ 191.2, 157.3 (q), 144.5 (q), 143.3 (q), 136.6 (q), 134.0 (q), 130.5, 129.2, 128.4, 127.7, 127.2, 125.8, 124.0, 21.7 (CH_3), 21.6 (CH_3), 19.9 (CH_3); HRMS (CI-TOF) calcd. for $C_{18}H_{18}O$+H m/z 251.1430, found 251.1425.

■ ASSOCIATED CONTENT

Supporting Information

Variable-temperature data plots for **2a**−**2g**; ^{1}H and ^{13}C NMR spectra for **2e**−**2g**, **5**, and **6**; Arrhenius plots and Eyring plots for **2a**−**2f**; selected crystallographic data and CIF file for **2g**; additional computational details; complete ref 44. This material is available free of charge via the Internet at http://pubs.acs.org.

■ AUTHOR INFORMATION

Corresponding Author

*E-mail: keith.ramig@baruch.cuny.edu (K.R.), edyta.greer@baruch.cuny.edu (E.M.G.), gopal.subramaniam@qc.cuny.edu (G.S.).

Notes

The authors declare no competing financial interest.

■ ACKNOWLEDGMENTS

We thank Dr. E. Fujita of Brookhaven National Laboratory for the use of the Bruker Kappa Apex II diffractometer for X-ray data collection. The experimental assistance of Nataliya Pokeza and Benjamin Kaplan is much appreciated. We thank the reviewers for their comments and for suggesting the method that allowed finding the transition state of compound **2g**. The Professional Staff Congress of the City University of New York is acknowledged for financial support of this work.

■ REFERENCES

(1) Eliel, E. E.; Wilen, S. H. *Stereochemistry of Carbon Compounds*; John Wiley and Sons: New York, 1994; pp 1119−1122 and 1166−1175.

(2) Mannschreck, A.; Rissmann, G.; Vögtle, F.; Wild, D. *Chem. Ber.* **1967**, *100*, 335−346.

(3) van Bergen, T. J.; Kellogg, R. M. *J. Org. Chem.* **1971**, *36*, 978−983.

(4) Katritzky, A. R.; Aurrecoechea, J. M.; Quian, K.; Koziol, A. E.; Palenik, G. J. *Heterocycles* **1987**, *25*, 387−391.

(5) Kowalski, D.; Erker, G.; Kotila, S. *Liebigs Ann.* **1996**, 887−890.

(6) Brooke, G. M.; Matthews, R. S. *J. Fluorine Chem.* **1988**, *40*, 109−117.

(7) Referring to ref 1, the (S_p) descriptor of the isomer on the left in Scheme 1 was assigned in the following way: C2 was chosen as the pilot atom, the atom of highest priority out of the plane formed by the benzo group plus C5 and N. From a viewpoint looking down on the molecule (i.e., so that C2 is between the viewer and the planar portion), the next three atoms from the pilot atom in order of priority are marked. Since these atoms, namely, N, C7, and C6, describe a counterclockwise turn, the (S_p) descriptor is assigned. The assignment is reversed when the molecule undergoes a ring-flip.

(8) Ramig, K.; Greer, E. M.; Szalda, D. J.; Razi, R.; Mahir, F.; Pokeza, N.; Wong, W.; Kaplan, B.; Lam, J.; Mannan, A.; Missak, C.; Mai, D.; Subramaniam, G.; Berkowitz, W. F.; Prasad, P.; Karimi, S.; Lo, N. H.; Kudzma, L. V. *Eur. J. Org. Chem.* **2010**, 2362−2371.

(9) Kudzma, L. V. *Synthesis* **2003**, 1661−1666.

(10) Blount, J. F.; Fryer, R. I.; Gilman, N. W.; Todaro, L. J. *Mol. Pharmacol.* **1983**, *24*, 425−428.

(11) Linscheid, P.; Lehn, J.-M. *Bull. Soc. Chim. Fr.* **1967**, 992−997.

(12) Sunjic, V.; Lisini, A.; Sega, A.; Kovac, T.; Kajfez, F.; Ruscic, B. *J. Heterocycl. Chem.* **1979**, *16*, 757−761.

(13) Paizs, B.; Simonyi, M. *Chirality* **1999**, *11*, 651−658.

(14) Carlier, P. R.; Zhao, H.; DeGuzman, J.; Lam, P. C.-H. *J. Am. Chem. Soc.* **2003**, *125*, 11482−11483.

(15) Lam, P. C.-H.; Carlier, P. *J. Org. Chem.* **2005**, *70*, 1530−1538.

(16) Carlier, P. R.; Zhao, H.; MacQuerrie-Hunter, S. L.; DeGuzman, J. C.; Hsu, D. C. *J. Am. Chem. Soc.* **2006**, *128*, 15215−15220.

(17) Carlier, P. R.; Sun, Y.-S.; Hsu, D. C.; Chen, Q.-H. *J. Org. Chem.* **2010**, *75*, 6588−6594.

(18) Lee, S.; Kamide, T.; Tabata, H.; Takahashi, H.; Shiro, M.; Natsugari, H. *Bioorg. Med. Chem.* **2008**, *16*, 9519−9523.

(19) Simonyi, M.; Maksay, G.; Kovacs, I.; Tegyey, Z.; Parkanyi, L.; Kalman, A.; Otvos, L. *Bioorg. Chem.* **1990**, *18*, 1−12.

(20) Fitos, I.; Visy, J.; Zsila, F.; Mady, G.; Simonyi, M. *Bioorg. Med. Chem.* **2007**, *15*, 4857−4862.

(21) Gilman, N. W.; Rosen, P.; Earley, J. V.; Cook, C.; Todaro, L. J. *J. Am. Chem. Soc.* **1990**, *112*, 3969−3978.

(22) Duffey, M. O.; Vos, T. J.; Adams, R.; Alley, J.; Anthony, J.; Barrett, C.; Bharathan, I.; Bowman, D.; Bump, N. J.; Chau, R.; Cullis, C.; Driscoll, D. L.; Elder, A.; Forsyth, N.; Frazer, J.; Guo, J.; Guo, L.; Hyer, M. L.; Janowick, D.; Kulkarni, B.; Lai, S.-J.; Lasky, K.; Li, G.; Li, J.; Liao, D.; Little, J.; Peng, B.; Qian, M. G.; Reynolds, D. J.; Rezaei, M.; Scott, M. P.; Sells, T. B.; Shinde, V.; Shi, Q. J.; Sintchak, M. D.; Soucy, F.; Sprott, K. T.; Stroud, S. G.; Nestor, M.; Visiers, I.; Weatherhead, G.; Ye, Y.; Damore, N. *J. Med. Chem.* **2012**, *55*, 197−208.

(23) Becker, A.; Kohfeld, S.; Lader, A.; Preu, L.; Pies, T.; Wieking, K.; Ferandin, Y.; Knockaert, M.; Meijer, L.; Kunick, C. *Eur. J. Med. Chem.* **2010**, *45*, 335−342.

(24) Seto, M.; Aikawa, K.; Miyamoto, N.; Aramaki, Y.; Kanzaki, N.; Takashima, K.; Kuze, Y.; Iizawa, Y.; Baba, M.; Shiraishi, M. *J. Med. Chem.* **2006**, *49*, 2037−2048.

(25) Jackson, P. F.; Davenport, T. W.; Garcia, L.; McKinney, J. A.; Melville, M. G.; Harris, G. G.; Chapdelaine, M. J.; Damewood, J. R.; Pullan, L. M.; Goldstein, J. M. *Bioorg. Med. Chem. Lett.* **1995**, *5*, 3097−3100.

(26) Cole, K. P.; Mitchell, D.; Carr, M. A.; Stout, J. R.; Belvo, M. D. *Tetrahedron: Asymmetry* **2009**, *20*, 1262−1266.

(27) Liu, P.; Lanza, T. J., Jr.; Chioda, M.; Jones, C.; Chobanian, H. R.; Guo, Y.; Chang, L.; Kelly, T. M.; Kan, Y.; Palyha, O.; Guan, X.-M.; Marsh, D. J.; Metzger, J. M.; Ramsay, K.; Wang, S.-P.; Strack, A. M.; Miller, R. J.; Pang, J.; Lyons, K.; Dragovic, J.; Ning, J. G.; Schafer, W. A.; Welch, C. J.; Gong, X.; Gao, Y.-D.; Hornak, V.; Ball, R. G.; Tsou, N.; Reitman, M. L.; Wyvratt, M. J.; Nargund, R. P.; Lin, L. S. *ACS Med. Chem. Lett.* **2011**, *2*, 933−937.

(28) Tabata, H.; Wada, N.; Takada, Y.; Oshitari, T.; Takahashi, H.; Natsugari, H. *J. Org. Chem.* **2011**, *76*, 5123−5131.

(29) Welch, C. J.; Gong, X.; Schafer, W.; Chobanian, H.; Lin, L.; Biba, M.; Liu, P.; Guo, Y.; Beard, A. *Chirality* **2009**, *21*, E105−E109.

(30) Oki, M. *Top. Stereochem.* **1983**, *14*, 1−81.

(31) Clayden, J. *Ang. Chem., Int. Ed.* **2009**, *48*, 6398−6401.

(32) Ramig, K.; Alli, S.; Cheng, M.; Leung, R.; Razi, R.; Washington, M.; Kudzma, L. V. *Synlett* **2007**, 2868−2870.

(33) Mukaiyama, T.; Narasaka, K. *Org. Synth.* **1987**, *65*, 6−11.

(34) Narasaka, K. *Org. Synth.* **1987**, *65*, 12−16.

(35) Streef, J. W.; van der Plas, H. C. *Tetrahedron Lett.* **1979**, 2287−2290.

(36) $\Delta G^{\ddagger}_c = 4.58\ T_c(10.32 + \log T_c/k_c)$ cal mol^{-1}. Here, T_c is the coalescence temperature and k_c is the exchange rate constant at the coalescence temperature. $k_c = \pi\Delta\nu/\sqrt{2}$, where $\Delta\nu$ is the separation of the two coalescing proton signals in Hz. See: Sandström, J. *Dynamic NMR Spectroscopy*; Academic Press: New York, 1982.

(37) Anna, J. M.; Ross, M. R.; Kubarych, K. J. *J. Phys. Chem. A* **2009**, *113*, 6544−6547.

(38) Weast, R., Ed. *CRC Handbook of Chemistry and Physics*, 62nd ed.; CRC Press: Boca Raton, FL, 1981−1982; p F−43.

(39) Anslyn, E. V.; Dougherty, D. A. *Modern Physical Organic Chemistry*; University Science Books: Herndon, VA, 2006; pp 370−371.

(40) Finner, E.; Zeugner, H.; Milkowski, W. *Arch. Pharm. (Weinheim, Ger.)* **1984**, *317*, 369−371.
(41) Finner, E.; Zeugner, H.; Milkowski, W. *Arch. Pharm. (Weinheim, Ger.)* **1984**, *317*, 1050−1053.
(42) Alebic-Kolbah, T.; Kajfez, F.; Rendic, S.; Sunjic, V. *Biochem. Pharmacol.* **1979**, *28*, 2457−2464.
(43) Konowal, A.; Snatzke, G.; Alebic-Kolbah, T.; Kajfez, F.; Rendic, S.; Sunjic, V. *Biochem. Pharmacol.* **1979**, *28*, 3109−3113.
(44) Frisch, M.; et al. *Gaussian 09*, Revision C.01. (See the Supporting Information for full citation.)
(45) Sheldrick, G. M. *Acta Crystallogr.* **2008**, *A64*, 112−122.